

## A Uniform Type Ia Supernova Distance Ladder with the Zwicky Transient Facility: Absolute Calibration Based on the Tip of the Red Giant Branch (TRGB) Method

SUHAIL DHAWAN,<sup>1</sup> ARIEL GOOBAR,<sup>2</sup> JOEL JOHANSSON,<sup>2</sup> IN SUNG JANG,<sup>3</sup> MICKAEL RIGAUULT,<sup>4</sup> LUKE HARVEY,<sup>5</sup>  
KATE MAGUIRE,<sup>5</sup> WENDY L. FREEDMAN,<sup>6</sup> BARRY F. MADORE,<sup>7</sup> JESPER SOLLERMAN,<sup>8</sup> AND YOUNG-LO KIM + BUILDERS<sup>9</sup>

<sup>1</sup>*Institute of Astronomy and Kavli Institute for Cosmology, University of Cambridge, Madingley Road, Cambridge CB3 0HA, UK*

<sup>2</sup>*The Oskar Klein Centre for Cosmoparticle Physics, Department of Physics, Stockholm University, SE-10691 Stockholm, Sweden*

<sup>3</sup>*Department of Astronomy & Astrophysics, University of Chicago, 5640 S. Ellis Avenue, Chicago, IL 60637, USA*

<sup>4</sup>*Univ Lyon, Univ Claude Bernard Lyon 1, CNRS/IN2P3, IP2I Lyon, UMR 5822, F-69622, Villeurbanne, France*

<sup>5</sup>*School of Physics, Trinity College Dublin, The University of Dublin, Dublin 2, Ireland*

<sup>6</sup>*Department of Astronomy & Astrophysics & Kavli Institute for Cosmological Physics, University of Chicago, 5640 South Ellis Avenue, Chicago, IL 60637, USA*

<sup>7</sup>*The Observatories of the Carnegie Institution for Science, 813 Santa Barbara St., Pasadena, CA 91101, USA*

<sup>8</sup>*The Oskar Klein Centre, Department of Astronomy, Stockholm University, SE-10691 Stockholm, Sweden*

<sup>9</sup>*Department of Physics, Lancaster University, Lancs LA1 4YB, UK*

### ABSTRACT

The current Cepheid distance ladder measurement of  $H_0$  is reported to be in tension with the values inferred from the cosmic microwave background (CMB), assuming standard model cosmology. However, the tip of the red giant branch (TRGB) reports an estimate of  $H_0$  in better agreement with the CMB. Hence, it is critical to reduce systematic uncertainties in local measurements to understand the origin of the Hubble tension. In this paper, we propose a uniform distance ladder, combining SNe Ia observed by the Zwicky Transient Facility (ZTF) with a TRGB calibration of their absolute luminosity. A large, volume-limited, sample of both calibrator and Hubble flow SNe Ia from the *same* survey minimizes two of the largest sources of systematics: host-galaxy bias and non-uniform photometric calibration. We present results from a pilot study using existing TRGB distance to the host galaxy of ZTF SN Ia SN 2021rhu (aka ZTF21abiuvdk). Combining the ZTF calibrator with a volume-limited sample from the first data release of ZTF Hubble flow SNe Ia, we infer  $H_0 = XX \pm 6.4 \text{ km s}^{-1} \text{ Mpc}^{-1}$ , an 8.3% measurement. The error budget is dominated by the single calibrator SN in this pilot study. However, the ZTF sample includes already five other SNe Ia within  $\sim 20$  Mpc for which TRGB distances can be obtained with HST. Finally, we present the prospects of building this distance ladder out to 80 Mpc with JWST observations of more than one hundred SNe Ia.

*Keywords:* cosmology: observations - supernovae

### 1. INTRODUCTION

Over the last decade, remarkable increase in accuracy obtained by a broad range of independent cosmological observations has provided compelling support for our current standard  $\Lambda$  cold dark matter ( $\Lambda$ CDM) model. This concordance cosmology successfully ex-

plains the measurements of fluctuations in the temperature and polarization of the cosmic microwave background (CMB) radiation (Planck Collaboration 2020) as well as observations of large-scale structure and matter fluctuations in the universe, e.g. baryon acoustic oscillations (BAO; Macaulay et al. 2019).

With improved accuracy of recent observations some discrepancies have been noted. The *prima facie* most significant tension is between the CMB inferred value of the Hubble constant ( $H_0$ ) and the direct measurement of the local value of  $H_0$  (Riess et al. 2021). The local measurements are based on a calibration of the absolute luminosity of Type Ia supernovae (SNe Ia) using independent distances to host galaxies of nearby SNe Ia, known

[suhail.dhawan@ast.cam.ac.uk](mailto:suhail.dhawan@ast.cam.ac.uk)

[ariel@fysik.su.se](mailto:ariel@fysik.su.se)

[joeljo@fysik.su.se](mailto:joeljo@fysik.su.se)

[m.rigault@ipnl.in2p3.fr](mailto:m.rigault@ipnl.in2p3.fr)

as the “cosmic distance ladder”. This claimed tension, if confirmed, it could provide evidence for of new fundamental physics beyond the standard model of cosmology. It could, however, be a sign of unknown sources of systematic error. Currently, the local  $H_0$  methods have slight differences in their values. The tip of the red giant branch (TRGB; Freedman 2021) and Cepheid (Riess et al. 2021) distance scales yield values of  $69.8 \pm 1.7$  and  $73.04 \pm 1.04 \text{ kms}^{-1}\text{Mpc}^{-1}$ , respectively. Understanding these differences is important to discerning whether the tension is a sign of novel physics or a yet-to-be-revealed systematic error. To date, only the TRGB and Cepheid measurements have measured distances to  $\mathcal{O}(10)$  host galaxies of SNe Ia.

Circumventing the two largest, known sources of systematic error is key to achieving the percent level precision in the local distance scale and resolving the Hubble tension. Firstly, Cepheid variables strongly prefer young, star-forming environments. This has been shown to bias the inferred SN Ia luminosity, and hence  $H_0$  (Rigault et al. 2020), though the size of this effect is currently debated (Jones et al. 2018). While the current Cepheid distance ladder addresses this issue by evaluating  $H_0$  from only the Hubble flow SNe Ia in low stellar mass hosts, it is important to measure  $H_0$  using a volume-limited calibrator and Hubble flow sample of SNe Ia in all types of host galaxies, given the profound cosmological implications of the Hubble tension. TRGBs, unlike Cepheid variables, are found in both old and young environments, hence, can probe SN Ia host galaxies of all morphological types in a given volume. The TRGB is a well-understood standard candle, arising from the core helium flash luminosity at the end phase of red giant branch (RGB) evolution for low-mass stars (Freedman et al. 2019; Jang et al. 2021; Freedman 2021). Furthermore, TRGB stars, found in the outskirts of galaxies, are less prone than Cepheids to biases from crowding, and are also comparatively less sensitive to reddening systematics, a potential contribution to the Cepheid  $H_0$  measurements (e.g., Mortsell et al. 2021).

Secondly, the current sample of SNe Ia for  $H_0$  measurements is derived from several ( $> 20$ ) different combinations of telescopes, instruments and filters (e.g. Scolnic et al. 2021; Riess et al. 2021). Although there have been significant efforts to cross-calibrate the heterogeneous systems (Brout et al. 2021), there are irreducible uncertainties associated with the data where the filters, instruments and *even telescopes* no longer exist. In light of these outstanding sources of error, it is imperative to have a volume limited sample of calibrator and Hubble flow SNe Ia observed with the *same* instrument.

Addressing these issues, here, we present a uniform distance ladder, with both calibrator and Hubble flow SNe Ia observed by the Zwicky Transient Facility (ZTF; Bellm et al. 2019; Graham et al. 2019), calibrated based on the TRGB method. As both calibrator and Hubble flow rungs of the distance ladder with the same instrument, we only rely on a relative photometric calibration, which is a significantly simpler task than controlling the absolute calibration of an SN Ia sample. In this pilot study, we present ZTF calibrator SNe Ia within a nearby volume of  $D_L < 20$  Mpc and measure preliminary distances, where possible, for those SNe Ia using tip of the red giant branch. In the long term, we need, assuming the current number of primary anchors, a ZTF calibrator sample of  $\sim 100$  SNe Ia to get to  $\sim 1\%$  precision and accuracy on  $H_0$  to resolve the tension. With the James Webb Space Telescope (JWST) scheduled to start taking data in mid-2022, we can feasibly extend the calibrator rung to  $D_L \sim 80$  Mpc. ZTF has already observed well-sampled light curves for more than one hundred SNe Ia in this distance range. Therefore, within the  $D_L \leq 80$  Mpc volume we will no longer be limited by the rate of SNe Ia in galaxies to obtain calibrator distances, currently a limiting factor for the largest calibrator sample (Riess et al. 2021).

## 2. DATA AND METHODOLOGY

We present the data for SNe Ia observed by ZTF in a  $D_L < 20$  Mpc volume, which also have a robust reported TRGB distances. While 5 SNe Ia have adequate light curve sampling to get precise peak magnitudes, shape and colour parameters from SNe Ia, only one of them, ZTF21abiuvdK (aka SN 2021rhu) has observations of the host galaxy to get an accurate distance.

SN 2021rhu exploded in NGC 7814, at coordinates,  $\alpha = 0.8143, \delta = 16.1457$ , classified as an SN Ia on the Transient Name Server (TNS; Munoz-Arancibia et al. 2021; SNIAscore 2021). We obtained photometry with a 1-day cadence for SN 2021rhu with ZTF, in the  $g, r, i$  filters between  $-14.1$  and  $+172.5$  days. These observations begin on July 1.404 2021 UTC. Hence, we obtained a densely sampled light curve with the ZTF observing system (Dekany et al. 2020), in multiple filters with the same system as the Hubble flow sample (as presented in Dhawan et al. 2022). The images were processed with the pipeline as detailed in Masci et al. (2019). The lightcurve, thus far, spans a large phase range from July 1.4 to November 11.11 2021. We have also obtained a well-sampled spectral time series, beginning with a classification spectrum with the SED-machine (Blagorodnova et al. 2018; Rigault et al. 2019) on 2021-07-05. These are presented in detail in a com-

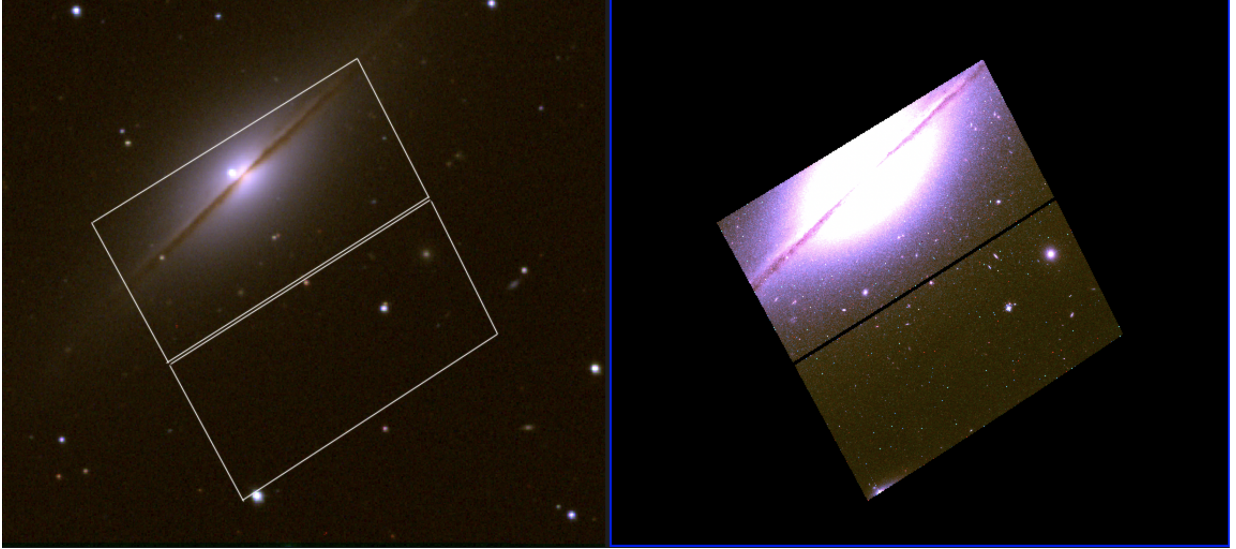


**Figure 1.** (Left) A combined red-green-blue image of SN 2021rhu from the ZTF data with one of the HST fields for the TRGB distance overplotted. (Right) A zoom in into the HST data of the host galaxy NGC 7814 Field 01 in the F606W filter with ACS.

157 panion paper (Harvey et al. in prep). Figure 2 shows  
 158 a maximum-light spectrum obtained with the SPectro-  
 159 graph for the Rapid Acquisition of Transients (SPRAT;  
 160 Piascik et al. 2014) on the Liverpool Telescope (LT;  
 161 Steele et al. 2004).

162 SNe Ia distances are inferred from light curve peak lu-  
 163 minosity, shape and colour. The most widely used light-  
 164 curve fitting algorithm, which we adopt for our analy-  
 165 sis, is the Spectral Adaptive Lightcurve Template - 2  
 166 (SALT2; Guy et al. 2007). This model treats the colour  
 167 entirely empirically, without distinguishing the intrinsic  
 168 and extrinsic components. We use the most updated,  
 169 published version of SALT2 (SALT2.4, see Guy et al.  
 170 2010; Betoule et al. 2014) as implemented in `sncosmo`  
 171 v2.1.0<sup>1</sup> (Barbary et al. 2016), identical to the lightcurve  
 172 inference of the Hubble flow sample in Dhawan et al.  
 173 (2022). In the fitting procedure, we correct the SN fluxes  
 174 for extinction due to dust in the Milky Way (MW). Ex-  
 175 tinction values for the SN coordinates derived in Schlafly  
 176 & Finkbeiner (2011) were applied, using the galactic  
 177 reddening law proposed in Cardelli et al. (1989), with a  
 178 total-to-selective absorption ratio,  $R_V = 3.1$ , the canon-  
 179 ical MW value.

### 2.1. TRGB distance estimate

181 NGC 7814 was observed with the Advanced Camera  
 182 for Surveys (ACS) on HST covering a total of seven fields  
 183 as part of the GHOSTS survey (Radburn-Smith et al.  
 184 2011). Here, we reanalyse the data using a pipeline by  
 185 the Carnegie-Chicago Hubble (CCHP; Freedman et al.

186 2019) program which implements its own point-spread  
 187 function (PSF) fitting photometry based on DOLPHOT  
 188 (Dolphin 2000) modeling synthetic PSFs with TinyTim  
 189 (Krist et al. 2011). The details of the pipeline can be  
 190 found in Jang et al. (2021). We select fields 3,4,5 from  
 191 the entire dataset since fields 1 and 2 are close to disk  
 192 of the galaxy and hence, susceptible to high crowding  
 193 and extinction, whereas fields 6 and 7 are very sparse  
 194 and hence, it is difficult to identify the TRGB. We per-  
 195 form artificial star tests by injecting 180,000 stars into  
 196 the FLC images and recover them using DOLPHOT.  
 197 The artificial stars have a similar colours range to blue  
 198 RGB stars of  $0.6 < F606W - F814W \leq 1.6$ . We pop-  
 199 ulate stars within a brightness range of  $25 < F814W \leq$   
 200  $29$  mag. To mimic the observed spatial distribution and  
 201 luminosity function (LF), we place more stars in the  
 202 inner region of the galaxy. The LF was binned with a  
 203 width of 0.01 mag and smoothed with a Gaussian kernel  
 204 of 0.1 mag. The edge detection is derived from the first  
 205 derivative of the scale smoothed LF (see Hatt et al. 2017,  
 206 for details). We find a Milky Way extinction corrected  
 207 tip at  $F814W_{\text{TRGB}} = 26.81 \pm 0.054$  mag. Details of the  
 208 tests, the impact of assumptions on the various com-  
 209 ponents of the pipeline and consistency with distances  
 210 reported in the literature are presented in a companion  
 211 paper (Jang 2022 in prep). Using the absolute calibra-  
 212 tion of the TRGB magnitude from multiple primary as  
 213 reported in Freedman (2021),  $M_{F814W}^{\text{TRGB}} = -4.049 \pm 0.038$   
 214 (see also, Li et al. 2022, for a new calibration from the  
 215 Milky Way) and we obtain a distance of  $\mu = 30.86 \pm 0.07$   
 216 mag.

<sup>1</sup> <https://sncosmo.readthedocs.io/en/v2.1.x/>

We combine the calibrator data with the ZTF DR1 Hubble flow sample (Dhawan et al. 2022). TRGB stars are found in all types of SN Ia host galaxies and therefore, the TRGB-calibrated sample will be volume limited. To have a completely volume-limited distance ladder, we also only fit the volume-limited Hubble flow sample from ZTF DR1. We conservatively take the sample to be complete to  $z \leq 0.06$ . This selection cut reduces the Hubble flow sample from 200 to 98 SNe Ia.

### 3. RESULTS

We fit the SALT2 light-curve model to the calibrator SN and get the peak luminosity, light-curve width and colour. We note that since SALT2 is not well defined at wavelengths redder than 7000 Å, we only fit the  $g$  and  $r$  filters (e.g. Jones et al. 2019). SN 2021rhu has SALT2 parameters  $m_B = 12.22 \pm 0.033$ , light-curve shape  $x_1 = -2.074 \pm 0.025$ , and colour,  $c = 0.054 \pm 0.028$ . While the  $x_1$  and  $c$  are within the range of typical cosmological cuts, it has a low  $x_1$  value which is also seen in peculiar, fast-declining SNe Ia. However, the light curves of SN 2021rhu show a clear shoulder in the  $r$  band and a second peak in the  $i$  band (Figure 2), characteristic of normal and transitional SNe Ia used for cosmology (Hsiao et al. 2015). We also compute the colour-stretch parameter,  $s_{BV}$ , with the SNooPY method, since it is shown to be better at parametrising the fast declining SNe Ia (Burns et al. 2014). We find  $s_{BV} = 0.72$  consistent with normal/transitional SNe Ia, appropriate to use for cosmology (Burns et al. 2018). It is also spectroscopically similar to transitional SNe Ia like SN 2011iv (Foley et al. 2012), which have been used for estimating  $H_0$  (Freedman et al. 2019), thus, this object is consistent with the cosmological sample of SNe Ia.

Here, we present the formalism for inferring  $H_0$ . The absolute magnitude of SNe Ia,  $M_B$ , is given by

$$m_B^0 - \mu_{\text{host}} = M_B \quad (1)$$

where  $m_B^0$  is the *standardized* apparent peak magnitude of the SN Ia and  $\mu_{\text{host}}$  is the distance modulus to the host galaxy based on the TRGB method. The Hubble flow SNe Ia measure the intercept of the magnitude-redshift relation,  $a_B$ . Ignoring higher order terms, the intercept is given by

$$a_B = \log cz + \log \left[ 1 + \frac{(1-q_0)z}{2} - \frac{(1-q_0-3q_0^2+j_0)z^2}{6} \right] - 0.2m_B^0. \quad (2)$$

We fix  $q_0$ ,  $j_0$  to the standard values of  $-0.55$  and  $1$  respectively, since the low- $z$  SN Ia sample alone cannot constrain them. We note that while cosmological studies with SNe Ia correct the redshifts for the Hubble flow sample accounting for peculiar motion due to

local large scale structure, this effect has been shown to be a sub-dominant source of error in measuring  $H_0$  (Peterson et al. 2021), which is especially true here since only a single calibrator dominates the error budget.  $m_B^0$  is expressed in terms of the light-curve parameters and corrections as

$$m_B^0 = m_B + \alpha x_1 - \beta c - \delta_{\mu\text{-bias}} \quad (3)$$

where  $\alpha$  and  $\beta$  are the slopes of the width-luminosity and colour-luminosity relations, respectively, and  $\delta_{\mu\text{-bias}}$  is the bias correction needed to account for selection effects and other sources of distance bias. Following the formalism of Brout et al. (2022), the canonical term for the host galaxy “mass-step” correction is absorbed in the bias correction  $\delta_{\mu\text{-bias}}$  (see also Brout & Scolnic 2021). Since both the calibrator described by equation 1 and the Hubble flow SNe Ia described by equation 2 are constructed to be volume-limited, such that they both have the *same* mass-step correction, the  $\delta_{\mu\text{-bias}}$  term will cancel out.

The error for each SN includes fit uncertainty from the SALT2 covariance matrix ( $\sigma_{\text{fit}}$ ), the peculiar velocity error ( $\sigma_{\text{pec}}$ ) and  $\sigma_{\text{int}}$ .

$$\sigma_m^2 = \sigma_{\text{fit}}^2 + \sigma_{\text{pec}}^2 + \sigma_{\text{int}}^2 \quad (4)$$

For  $\sigma_{\text{pec}}$  we derive the magnitude error from a velocity error of  $300 \text{ km s}^{-1}$  (Carrick et al. 2015) We use PyMultiNest (Buchner et al. 2014), a python wrapper for MultiNest (Feroz et al. 2009) to derive the posterior distribution on the parameters. With the current calibrator, we find,  $H_0 = XX \pm 6.4 \text{ km s}^{-1} \text{ Mpc}^{-1}$ . We also fit for  $H_0$  using the entire Hubble flow DR1 sample and find  $H_0 = YY \pm 6.0 \text{ km s}^{-1} \text{ Mpc}^{-1}$ , a small difference of  $0.65 \text{ km s}^{-1} \text{ Mpc}^{-1}$ . This uncertainty is not significantly smaller when using the entire gold sample for ZTF DR1 compared to the volume limited one. This is because the main source of uncertainty is from having on a single calibrator object.

We also infer the corrected peak magnitudes with SNooPy (Burns et al. 2014). While SNooPy uses a light-curve template as opposed to a spectral template for SALT2, it is trained with a larger sample of transitional SNe Ia similar to SN 2021rhu, hence, we compare  $H_0$  values from both methods. We compute distances to both the Hubble flow SNe Ia and SN 2021rhu with the EBV\_model12. Using the same analysis method for the SALT2 fitted distances, we infer an  $H_0$  value of  $YY \pm 6.1 \text{ km s}^{-1} \text{ Mpc}^{-1}$ , a difference of  $0.65 \text{ km s}^{-1} \text{ Mpc}^{-1}$  from the value using SALT2. This difference is significantly smaller than the uncertainty on  $H_0$  from either method. Moreover, since SNooPy has a well-sampled training set to build the  $i$ -band template

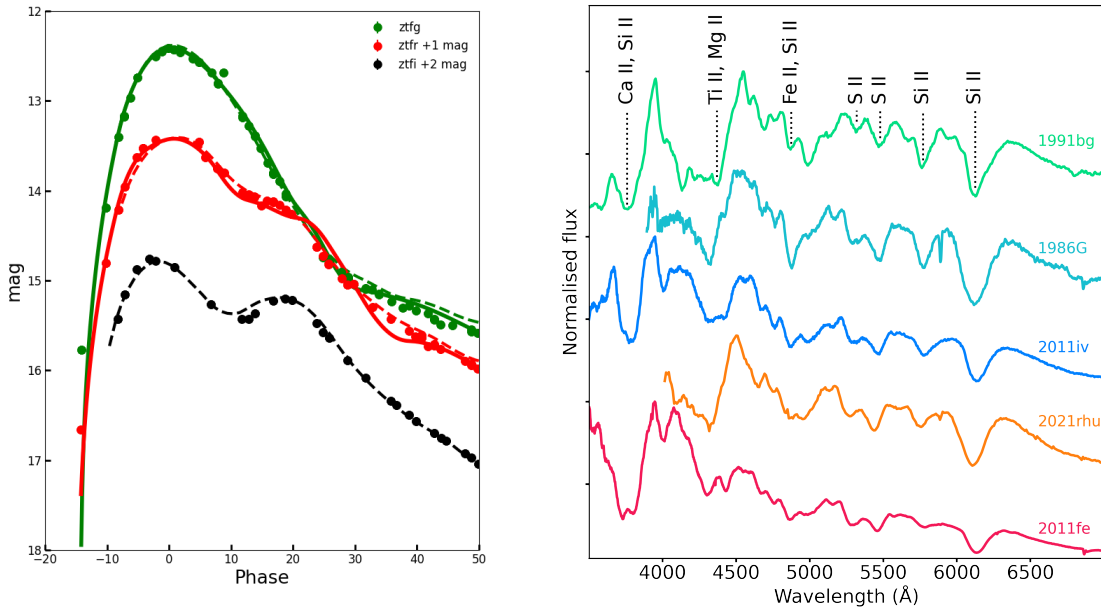


**Figure 2.** (Left): Lightcurve of SN 201rhu in the  $g, r, i$  filters (filled circles) along with the SALT2 model fit to the  $g, r$  filters overplotted (solid) and the SNOoPy model fit to the  $g, r, i$  filters (dashed). The plot has truncated this the phase at which the SALT2 model is defined. (Right) A maximum light spectrum of SN 201rhu (orange), in comparison with the peculiar, subluminal SN 1991bg (green; Filippenko et al. 1992), transitional SN 1986G (cyan; Cristiani et al. 1992) and SN 2011iv (blue; Foley et al. 2012), the latter has been used as a calibrator object and the normal SN 2011fe (red; Parent et al. 2012). The most common spectral features of intermediate mass and iron group elements of SNe Ia at maximum light are shown as dotted lines. We find that the near maximum light spectrum of SN 201rhu is very similar to transitional SNe Ia (see also Harvey et al. in prep.)

we also infer  $H_0$  from the  $g, r, i$  filter combination and find a value of  $YY \pm 6.0 \text{ km s}^{-1} \text{ Mpc}^{-1}$ , a difference of  $0.684 \text{ km s}^{-1} \text{ Mpc}^{-1}$  from the fiducial case.

#### 4. DISCUSSION AND CONCLUSION

We present an estimate of  $H_0$  from a uniform distance ladder using the same survey for the calibrator sample as a homogeneous, untargeted Hubble flow sample. We use a TRGB distance to a nearby host galaxy of an SN Ia with high-cadence data in the ZTF  $g, r, i$  filters. The current uncertainty is not sufficient to weigh in on the Hubble tension. We note that even a factor of 2 reduction in the Hubble flow sample by imposing the volume limit does not impact the uncertainty on  $H_0$  the error currently is driven by the low number of ZTF SNe Ia with robust, independent distances. However, this can be increased with HST observations for nearby host galaxies. In the  $D_L < 20 \text{ Mpc}$  volume, one where we can achieve completeness relatively quickly, there are 5 more SNe Ia with well-sampled light curves, a sample expected to increase by  $\sim 1 - 2$  per year for the remainder of ZTF. These SNe are

1. ZTF19aacgslb (SN 2019np) in NGC 3254

2. ZTF20abijfqq (SN 2020nlb) in NGC 4382 (M85)
3. ZTF20abrjmg (SN 2020qxp) in NGC 5002
4. ZTF21aaabvit (SN 2021J) in NGC 4414
5. ZTF21aaqytjr (SN 2021hiz) in UGC 7513

All the SNe Ia listed above have coverage in the  $g, r, i$  filters beginning from at least two weeks before maximum light and extending beyond +70 days. We note that even this small volume sample, there are early-type host galaxies like NGC 4382, for which other methods like Cepheid variables are not viable to obtain distances. In this volume, the number of calibrator SNe Ia is limited by the rate of SNe Ia exploding in the universe. The ZTF calibrator sample within the 20 Mpc volume, accumulated till date, is however, sufficient to measure  $H_0$  to  $\sim 3\%$  accuracy using only HST for TRGB observations. In our analyses, we only infer the SN Ia light-curve parameters using  $g$  and  $r$  filters since SALT2 is not optimal for redder wavebands. In future studies, we will implement improved SNe Ia models, e.g. SALT3 (Kenworthy et al. 2021), trained with high-cadence ZTF SN Ia data in the redder wavebands to measure SN Ia distances.

Future TRGB observations with the near infrared camera (NIRCam) on JWST can extend the calibra-

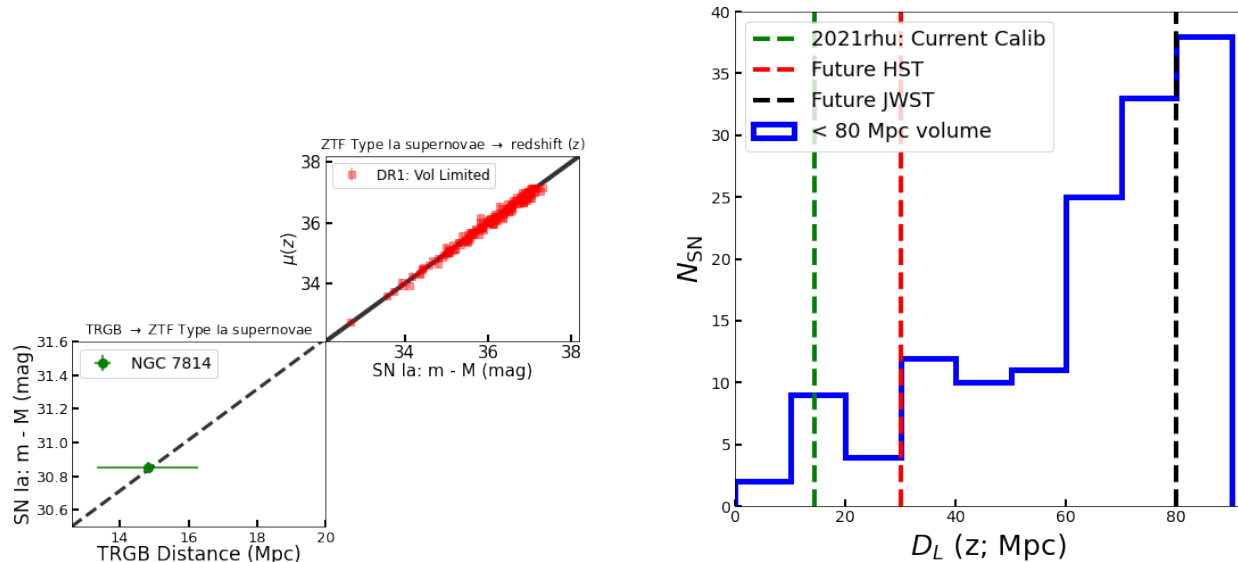


**Figure 3.** (Left): The current ZTF distance ladder with SN 2021rhu in NGC 7814 (green; the TRGB distance is plotted in linear scale instead of a distance modulus) and the Volume Limited Hubble flow sample from ZTF DR1 (red). We emphasize that all SNe Ia in this distance ladder are observed with the same survey. (Right): Histogram of luminosity distances for nearby ( $z \leq 0.02$ ) ZTF SNe Ia with sufficient observations infer distances. Distances are computed from the redshift assuming standard cosmology from Planck Collaboration et al. (2020) with  $H_0 = 67.4 \text{ km s}^{-1} \text{ Mpc}^{-1}$  and  $q_0, j_0$  of -0.55 and 1 respectively. Hence, they are only indicative. The distance for the current calibrator and the maximum distance feasible with HST and JWST are plotted as green, red and black vertical dashed lines respectively. There is a total of 114 SNe Ia with high-quality light curves in this volume, providing a large sample to build a ZTF-only distance ladder.

357 tor sample volume out to larger distances of up to 80  
 358 Mpc. In the volume  $20 < D_L < 80$  Mpc, we have high-  
 359 cadence light curves of 106 more SNe Ia already obtained  
 360 (see Figure 3), expected to increase by the end of ZTF.  
 361 Therefore, the complete sample of ZTF SNe Ia in a vol-  
 362 ume where JWST observations are feasible can increase  
 363 the current calibrator sample by a factor of  $\sim 2 - 3$ . We  
 364 emphasize that current SN Ia cosmology requires cross-  
 365 calibrating several heterogeneous photometric systems  
 366 (Brout et al. 2021). To get to percent level precision,  
 367 it is an important cross-check to have observations of a  
 368 large sample of SNe Ia on a single photometric system,  
 369 that is the *same* for calibrator and Hubble flow SNe Ia.  
 370 Hence, the increased statistical power and reduced sys-  
 371 tematic uncertainties from a single, untargeted survey,  
 372 make this an ideal approach to resolve the  $H_0$  tension.

### ACKNOWLEDGEMENTS

374 Based on observations obtained with the Samuel  
 375 Oschin Telescope 48-inch and the 60-inch Telescope at  
 376 the Palomar Observatory as part of the Zwicky Tran-  
 377 sient Facility project. ZTF is supported by the National  
 378 Science Foundation under Grant No. AST-2034437 and  
 379 a collaboration including Caltech, IPAC, the Weizmann  
 380 Institute for Science, the Oskar Klein Center at Stock-

381 holm University, the University of Maryland, Deutsches  
 382 Elektronen-Synchrotron and Humboldt University, the  
 383 TANGO Consortium of Taiwan, the University of Wis-  
 384 consin at Milwaukee, Trinity College Dublin, Lawrence  
 385 Livermore National Laboratories, IN2P3, France, the  
 386 University of Warwick, the University of Bochum, and  
 387 Northwestern University. Operations are conducted by  
 388 COO, IPAC, and UW. SEDMachine is based upon work  
 389 supported by the National Science Foundation under  
 390 Grant No. 1106171. SD acknowledges support from  
 391 the Marie Curie Individual Fellowship under grant ID  
 392 890695 and a JRF at Lucy Cavendish College. AG ac-  
 393 knowledges support from the Swedish Research Council  
 394 under Dnr VR 2020-03444 and the Swedish National  
 395 Space Board. This project has received funding from  
 396 the European Research Council (ERC) under the Eu-  
 397 ropean Union’s Horizon 2020 research and innovation  
 398 program (grant agreement n 759194 - USNAC). Y.-L.K.  
 399 acknowledges support by the Science and Facilities Re-  
 400 search Council [grant number ST/V000713/1]. WLF ac-  
 401 knowledges support from program #13691 provided by  
 402 NASA through a grant from the Space Telescope Science  
 403 Institute, which is operated by the Association of Uni-

404 versities for Research in Astronomy, Inc., under NASA  
 405 contract NASA 5-26555.

## REFERENCES

- 406 Barbary, K., Barclay, T., Biswas, R., et al. 2016, SNCosmo:  
 407 Python library for supernova cosmology.  
 408 <http://ascl.net/1611.017>
- 409 Bellm, E. C., Kulkarni, S. R., Graham, M. J., et al. 2019,  
 410 PASP, 131, 018002, doi: [10.1088/1538-3873/aaecbe](https://doi.org/10.1088/1538-3873/aaecbe)
- 411 Betoule, M., Kessler, R., Guy, J., et al. 2014, A&A, 568,  
 412 A22, doi: [10.1051/0004-6361/201423413](https://doi.org/10.1051/0004-6361/201423413)
- 413 Blagorodnova, N., Neill, J. D., Walters, R., et al. 2018,  
 414 PASP, 130, 035003, doi: [10.1088/1538-3873/aaa53f](https://doi.org/10.1088/1538-3873/aaa53f)
- 415 Brout, D., & Scolnic, D. 2021, ApJ, 909, 26,  
 416 doi: [10.3847/1538-4357/abd69b](https://doi.org/10.3847/1538-4357/abd69b)
- 417 Brout, D., Taylor, G., Scolnic, D., et al. 2021, arXiv  
 418 e-prints, arXiv:2112.03864.  
 419 <https://arxiv.org/abs/2112.03864>
- 420 Brout, D., Scolnic, D., Popovic, B., et al. 2022, arXiv  
 421 e-prints, arXiv:2202.04077.  
 422 <https://arxiv.org/abs/2202.04077>
- 423 Buchner, J., Georgakakis, A., Nandra, K., et al. 2014,  
 424 A&A, 564, A125, doi: [10.1051/0004-6361/201322971](https://doi.org/10.1051/0004-6361/201322971)
- 425 Burns, C. R., Stritzinger, M., Phillips, M. M., et al. 2014,  
 426 ApJ, 789, 32, doi: [10.1088/0004-637X/789/1/32](https://doi.org/10.1088/0004-637X/789/1/32)
- 427 Burns, C. R., Parent, E., Phillips, M. M., et al. 2018, ApJ,  
 428 869, 56, doi: [10.3847/1538-4357/aae51c](https://doi.org/10.3847/1538-4357/aae51c)
- 429 Cardelli, J. A., Clayton, G. C., & Mathis, J. S. 1989, ApJ,  
 430 345, 245, doi: [10.1086/167900](https://doi.org/10.1086/167900)
- 431 Carrick, J., Turnbull, S. J., Lavaux, G., & Hudson, M. J.  
 432 2015, MNRAS, 450, 317, doi: [10.1093/mnras/stv547](https://doi.org/10.1093/mnras/stv547)
- 433 Cristiani, S., Cappellaro, E., Turatto, M., et al. 1992, A&A,  
 434 259, 63
- 435 Dekany, R., Smith, R. M., Riddle, R., et al. 2020, PASP,  
 436 132, 038001, doi: [10.1088/1538-3873/ab4ca2](https://doi.org/10.1088/1538-3873/ab4ca2)
- 437 Dhawan, S., Goobar, A., Smith, M., et al. 2022, MNRAS,  
 438 510, 2228, doi: [10.1093/mnras/stab3093](https://doi.org/10.1093/mnras/stab3093)
- 439 Dolphin, A. E. 2000, PASP, 112, 1383, doi: [10.1086/316630](https://doi.org/10.1086/316630)
- 440 Feroz, F., Hobson, M. P., & Bridges, M. 2009, MNRAS,  
 441 398, 1601, doi: [10.1111/j.1365-2966.2009.14548.x](https://doi.org/10.1111/j.1365-2966.2009.14548.x)
- 442 Filippenko, A. V., Richmond, M. W., Branch, D., et al.  
 443 1992, AJ, 104, 1543, doi: [10.1086/116339](https://doi.org/10.1086/116339)
- 444 Foley, R. J., Kromer, M., Howie Marion, G., et al. 2012,  
 445 ApJL, 753, L5, doi: [10.1088/2041-8205/753/1/L5](https://doi.org/10.1088/2041-8205/753/1/L5)
- 446 Freedman, W. L. 2021, ApJ, 919, 16,  
 447 doi: [10.3847/1538-4357/ac0e95](https://doi.org/10.3847/1538-4357/ac0e95)
- 448 Freedman, W. L., Madore, B. F., Hatt, D., et al. 2019, ApJ,  
 449 882, 34, doi: [10.3847/1538-4357/ab2f73](https://doi.org/10.3847/1538-4357/ab2f73)
- 450 Graham, M. J., Kulkarni, S. R., Bellm, E. C., et al. 2019,  
 451 PASP, 131, 078001, doi: [10.1088/1538-3873/ab006c](https://doi.org/10.1088/1538-3873/ab006c)
- 452 Guy, J., Astier, P., Baumont, S., et al. 2007, A&A, 466, 11,  
 453 doi: [10.1051/0004-6361:20066930](https://doi.org/10.1051/0004-6361:20066930)
- 454 Guy, J., Sullivan, M., Conley, A., et al. 2010, A&A, 523,  
 455 A7, doi: [10.1051/0004-6361/201014468](https://doi.org/10.1051/0004-6361/201014468)
- 456 Hatt, D., Beaton, R. L., Freedman, W. L., et al. 2017, ApJ,  
 457 845, 146, doi: [10.3847/1538-4357/aa7f73](https://doi.org/10.3847/1538-4357/aa7f73)
- 458 Hsiao, E. Y., Burns, C. R., Contreras, C., et al. 2015, A&A,  
 459 578, A9, doi: [10.1051/0004-6361/201425297](https://doi.org/10.1051/0004-6361/201425297)
- 460 Jang, I. S., Hoyt, T. J., Beaton, R. L., et al. 2021, ApJ,  
 461 906, 125, doi: [10.3847/1538-4357/abc8e9](https://doi.org/10.3847/1538-4357/abc8e9)
- 462 Jones, D. O., Riess, A. G., Scolnic, D. M., et al. 2018, ApJ,  
 463 867, 108, doi: [10.3847/1538-4357/aae2b9](https://doi.org/10.3847/1538-4357/aae2b9)
- 464 Jones, D. O., Scolnic, D. M., Foley, R. J., et al. 2019, ApJ,  
 465 881, 19, doi: [10.3847/1538-4357/ab2bec](https://doi.org/10.3847/1538-4357/ab2bec)
- 466 Kenworthy, W. D., Jones, D. O., Dai, M., et al. 2021, arXiv  
 467 e-prints, arXiv:2104.07795.  
 468 <https://arxiv.org/abs/2104.07795>
- 469 Krist, J. E., Hook, R. N., & Stoehr, F. 2011, in Society of  
 470 Photo-Optical Instrumentation Engineers (SPIE)  
 471 Conference Series, Vol. 8127, Optical Modeling and  
 472 Performance Predictions V, ed. M. A. Kahan, 81270J,  
 473 doi: [10.1117/12.892762](https://doi.org/10.1117/12.892762)
- 474 Li, S., Casertano, S., & Riess, A. G. 2022, arXiv e-prints,  
 475 arXiv:2202.11110. <https://arxiv.org/abs/2202.11110>
- 476 Macaulay, E., Nichol, R. C., Bacon, D., et al. 2019,  
 477 MNRAS, 486, 2184, doi: [10.1093/mnras/stz978](https://doi.org/10.1093/mnras/stz978)
- 478 Masci, F. J., Laher, R. R., Rusholme, B., et al. 2019,  
 479 PASP, 131, 018003, doi: [10.1088/1538-3873/aae8ac](https://doi.org/10.1088/1538-3873/aae8ac)
- 480 Mortsell, E., Goobar, A., Johansson, J., & Dhawan, S.  
 481 2021, arXiv e-prints, arXiv:2105.11461.  
 482 <https://arxiv.org/abs/2105.11461>
- 483 Munoz-Arancibia, A., Mourao, A., Forster, F., et al. 2021,  
 484 Transient Name Server Discovery Report, 2021-2265, 1
- 485 Parrent, J. T., Howell, D. A., Friesen, B., et al. 2012, ApJL,  
 486 752, L26, doi: [10.1088/2041-8205/752/2/L26](https://doi.org/10.1088/2041-8205/752/2/L26)
- 487 Peterson, E. R., Kenworthy, W. D., Scolnic, D., et al. 2021,  
 488 arXiv e-prints, arXiv:2110.03487.  
 489 <https://arxiv.org/abs/2110.03487>

- 490 Piascik, A. S., Steele, I. A., Bates, S. D., et al. 2014, in  
491 Society of Photo-Optical Instrumentation Engineers  
492 (SPIE) Conference Series, Vol. 9147, Ground-based and  
493 Airborne Instrumentation for Astronomy V, ed. S. K.  
494 Ramsay, I. S. McLean, & H. Takami, 91478H,  
495 doi: [10.1117/12.2055117](https://doi.org/10.1117/12.2055117)
- 496 Planck Collaboration. 2020, A&A, 641, A6,  
497 doi: [10.1051/0004-6361/201833910](https://doi.org/10.1051/0004-6361/201833910)
- 498 Planck Collaboration, Aghanim, N., Akrami, Y., et al.  
499 2020, A&A, 641, A1, doi: [10.1051/0004-6361/201833880](https://doi.org/10.1051/0004-6361/201833880)
- 500 Radburn-Smith, D. J., de Jong, R. S., Seth, A. C., et al.  
501 2011, ApJS, 195, 18, doi: [10.1088/0067-0049/195/2/18](https://doi.org/10.1088/0067-0049/195/2/18)
- 502 Riess, A. G., Yuan, W., Macri, L. M., et al. 2021, arXiv  
503 e-prints, arXiv:2112.04510.  
504 <https://arxiv.org/abs/2112.04510>
- 505 Rigault, M., Neill, J. D., Blagorodnova, N., et al. 2019,  
506 A&A, 627, A115, doi: [10.1051/0004-6361/201935344](https://doi.org/10.1051/0004-6361/201935344)
- 507 Rigault, M., Brinnet, V., Aldering, G., et al. 2020, A&A,  
508 644, A176, doi: [10.1051/0004-6361/201730404](https://doi.org/10.1051/0004-6361/201730404)
- 509 Schlafly, E. F., & Finkbeiner, D. P. 2011, ApJ, 737, 103,  
510 doi: [10.1088/0004-637X/737/2/103](https://doi.org/10.1088/0004-637X/737/2/103)
- 511 Scolnic, D., Brout, D., Carr, A., et al. 2021, arXiv e-prints,  
512 arXiv:2112.03863. <https://arxiv.org/abs/2112.03863>
- 513 SNIascore. 2021, Transient Name Server Classification  
514 Report, 2021-2331, 1
- 515 Steele, I. A., Smith, R. J., Rees, P. C., et al. 2004, in  
516 Society of Photo-Optical Instrumentation Engineers  
517 (SPIE) Conference Series, Vol. 5489, Ground-based  
518 Telescopes, ed. J. Oschmann, Jacobus M., 679–692,  
519 doi: [10.1117/12.551456](https://doi.org/10.1117/12.551456)